Detection and Localization of CDM like ESD using a novel Sensor derived from Leaky-Coax

Gabriel Fellner
Institute of Electronics
Graz University of Technology
Graz, Austria
gabriel.fellner@tugraz.at

Amin Pak
Institute of Electronics
Graz University of Technology
& SAL Graz EMC lab
Graz, Austria
amin.pak@tugraz.at

David Pommerenke
Institute of Electronics
Graz University of Technology
& SAL Graz EMC lab
Graz, Austria
david.pommerenke@tugraz.at

***Abstract*—Downscaled semiconductors are at risk of CDM like ESD events during manufacturing, packaging, testing and placement. The reduction in silicon area spent for ESD protection circuits in modern ICs makes the devices more vulnerable by reducing damaging thresholds. Following this trend in industry it is getting more crucial to monitor ESD in processes where these devices are handled. A new type of sensor using multiple antennas along a coax-cable is used to locate CDM like ESD events. Due to the large quantity of antennas, this sensor has the potential to be used in more complex environments where a line of sight is not necessary for all antennas. The localization is performed based on an algorithm which compares the measured signal with a reference dataset from simulation. A hardware implementation together with a stepwise derivation of the algorithm is described. Evaluation of the system in an initial setup is showing encouraging performance for the localization.**

Keywords—Electrostatic discharge, CDM ESD, ESD localization

I. Introduction

Electronic manufacturing sites typically involve processes as un-taping of components, inserting components into placement machines, robotically moving components and finally placing them on a printed circuit board (PCB). Many of these steps before component placement involve mechanical movements which can lead to charge separation (triboelectric charging). In case a electrostatic charged component is placed on a board, the component will experience large currents and electric fields. This type of ESD event is commonly referred to charged device model (CDM) like ESD, which may or may not result in damage to the component. Since the risk is known by manufacturers, precautions are taken. Air ionizer, grounding of all mechanic parts, usage of materials which have favorable triboelectric charging properties are some of the established measures.

The reduction of transistor size in semiconductor devices forces a reduction of CDM and HBM protection levels [1]. For high speed, single nanometer devices CDM protection is often reduced to 125 V and it will fall with the increase of heterogenous integration. Thus the need for detecting and localizing even small CDM like events is increasing. A further challenge lies in the background noise levels within manufacturing, testing and packaging environments. A multitude of harmless pulses, e.g., from surface discharges, relays etc. may cover critical CDM events. Those background noise levels will not reduce, increasing the difficulty of CDM detection.

Different methods are available to spot the process step, where the damage occurs. The methods include measurements of static electric fields, measurement of charge on devices and also measurement of radiated electromagnetic interference (EMI) of the actual ESD event [2], [3]. Since static charge can be present on parts, without causing problems as ESD, the measurement of electromagnetic waves radiated by the discharge itself spots the problematic location.

A simple way to detect discharge events is by EMI detectors, which can also give some amount of information about the discharge, such as discharge type, RSSI, strength (if distance to event is known) [4]. By using three EMI detectors at known locations for the detection, the spatial position of the ESD can be determined by triangulation using the RSSI values [5].

In more advanced systems, multiple antennas in combination with fast sampling oscilloscopes are used instead of EMI detectors. This allows triangulation based on RSSI and a reverse global positioning system (GPS) approach using time of arrival (TOA). These systems show spatial resolutions down to 1 cm within areas of 3 m x 3 m [6]–[8]. These systems are only accurate when using the line of sight signals. The application is difficult in complex machinery, where a line of sight to each antenna is usually not possible. An example would be a large industrial pick and place machine.

To overcome this issue, the number of antennas can be increased. This increases the chance, that some antennas receive the radiated signals directly. The major drawback, which prevents an excessive increase in the number of antennas, is that each antenna requires an oscilloscope channel with sampling rates above 5 GSa/s.

In this paper we introduce a new sensor concept, which allows the usage of multiple antennas for CDM like ESD event localization, by only using two oscilloscope channels. The algorithm applied for the localization is not based on triangulation using RSSI or TOA, but on the correlation of measured data, with data gained from an LT-SPICE model of the sensor.

II. Architecture

A. Principle of the Sensor

The goal of the sensor structure is to increase the number of antennas, so the chance of picking up EMI from ESD events is larger even in complex environment. This should allow locating the ESD even in complex environment. By connecting multiple antennas along a coax cable no additional oscilloscope channels are required for receiving signals of those antennas. The main challenges in this connection of antennas along the cable:

- Overlap of received signals

- Mismatch and load of antenna
- Common mode currents on coax-shield
- Losses

There are two different cases which lead to overlapping signals. On the one hand, the received signals overlap, if the propagation delay in the coax-cable between the antennas is shorter than the width of the received signal. While on the other hand an overlap also occurs for very short signal if the wave in air travels in the same direction as the wave inside the coaxial-cable. This overlap is systematic and has to be treated in the data processing. A mathematical definition for the time difference between the signals of two antennas is given by:

$$t_{dAB} = \frac{\|\vec{r}_{B\,ESD}\| - \|\vec{r}_{A\,ESD}\|}{c} + \frac{L_{coax\,AB}}{c\,v_f} \qquad (1)$$

With $\vec{r}_{A\,ESD}$ and $\vec{r}_{B\,ESD}$ as the vector to the corresponding antenna A, B. c the speed of light, $L_{coax\,AB}$ the length of the coaxial cable between A and B. t_{dAB} as the delay between antenna A and B. v_f is the velocity factor of the cable describing how fast the signal propagates inside the cable. t_{dAB} is the time that the signal at antenna B is delayed in reference to antenna A. Fig. 1 shows the overlap behavior for an arrangement of three antennas as shown in the picture. The signal of antenna 1 is received first since the wave-propagation in air is faster than in the cable. Further it can be seen, that the signals of antenna 1 and 2 overlap because of the geometry. Signal 2 and 3 separated only the time delay of the cable, because they are in equal distance to the ESD.

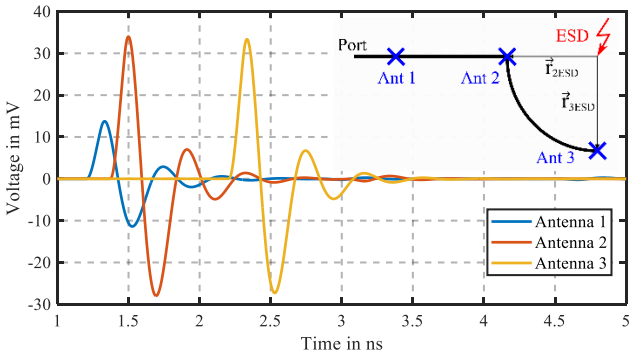

Fig. 1 LT-Spice simulation result for the antenna arrangement shown in the picture. A velocity factor of 0.8 is used for the cable, losses have been neglected in this simulation

Each antenna introduces a small mismatch and a load to signals propagating trough the coax-cable. Both are determined by the input impedance of the antenna. Using a 1 kΩ resistor leads to small mismatch, but reduces antenna sensitivity. If needed, each antenna could contain a LNA and couple into the coax cable via a high value resistor or a Schottky diode, such that the diode forms a very small capacitor when no signal is present but injects a pulse once the pulse amplitude at the output of the LNA surpasses 0.3 V.

The electromagnetic wave radiating from the ESD event is not only received at the antenna, but can also travels as a common mode current on the shield of the coax cable. This current along the shield additionally induces signals at the antennas. If this is the case, the 1/R field die-off in far field, cannot longer be observed in the amplitudes. Antennas in larger distance are able to deliver larger signals induced by the common mode current on the shield. This unwanted property is difficult to model and needs to be suppressed.

The large bandwidth of the system and the high pass characteristics of the antennas, see Fig. 5, allows to suppress none CDM style background pulses and allows to use spectral decomposition to further distinguish pulses.

B. Sensor Implementation

An easy and effective way of implementation of the antennas along the cable, is to directly implant the antennas in the cable. The antennas are somewhat monopole antennas, built of a 2 cm long wire. In order to minimize reflections and loading, a series resistor with a value of 1 kΩ is used at the antenna. This attenuates signals received at the antenna. Since the antenna has only the shield of the coax-cable as ground reference and a large series resistance, it can be treated more as a broadband D-Dot antenna than a monopole antenna. By implanting the antennas non-equidistant, a notch-filter characteristic is avoided. Conductive fabrics has been wrapped around the cable in between the antennas, to suppress common mode currents on the shield.

Fig. 2 shows the structure of the sensor. The antennas are 1 kΩ THT resistors with a length of 2 cm. These are inserted to holes, drilled into the coax-cable to the inner conductor. An ohmic connection to the inner conductor is made by silver paint. The distance between the antennas is varied in a range of 20 cm ±3 cm. A coaxial cable with a velocity factor of 80 % is used.

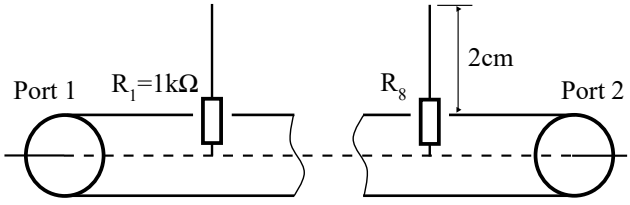

Fig. 2 Implementation of the sensor using a coaxial-cable. Small holes are drilled into the shield to reach the inner pin. Resistors are implanted using silverpaint. Overall 8 antennas are used in non-equidistant spacing of 20 cm ±3 cm.

The insertion loss of the sensor is shown in Fig. 3. No extra effort has been given to improve the S21. Using low loss cables and better workmanship the attenuation can be reduced. By using low capacitance TVS diodes instead of 1 kΩ resistors the insertion loss could be improved further.

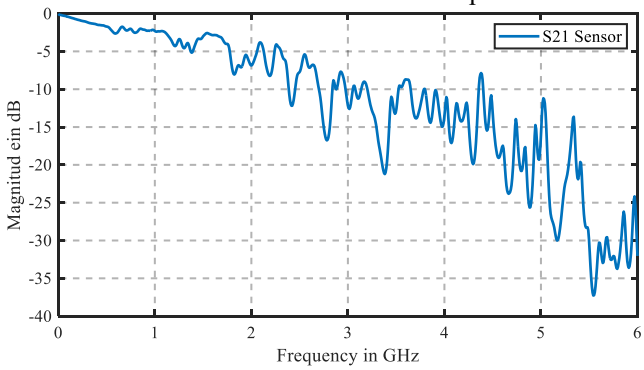

Fig. 3 Insertion loss of a prototype coax-cable sensor measured from port 1 to port 2

C. Antenna Characterization and Modeling

The antennas of the sensor have a derivative frequency response, above a certain frequency the derivative behavior is

compensated by "self-integration". This self-integration starts at the frequency where the majority of induced current will flow through the capacitance at the antenna. The voltage signal at the antenna is mostly determined by the frequency spectrum, polarization and amplitude of the field radiated by the ESD. In order to generate a lumped element SPICE model of the antenna, the frequency behavior is obtained from full-wave simulation using the software CST. Therefor a plane-wave was applied to one antenna of the coax-cable. For this simulation the cable was models according to the geometry and electrical characteristic of the datasheet. A simulated characteristic impedance of 51 Ω verifies this model. Fig. 4 shows the simulation setup, whereby the polarization of the plane wave was in y-direction, which is the favorable polarization of the antenna. The resulting characteristic is shown in Fig. 5.

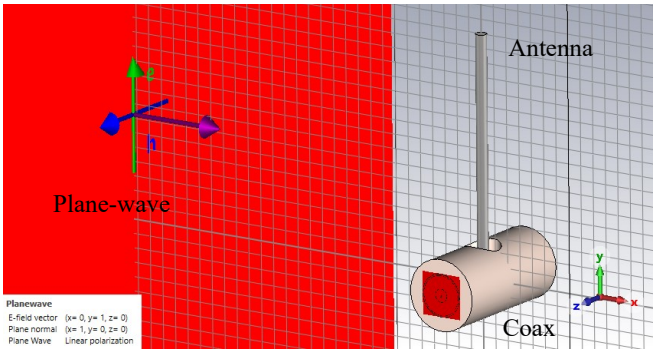

Fig. 4 Full-wave simulation setup for plane-wave simulation. Both ends of the coaxial-cable are terminated using a wave-port. The antenna is connected to the inner conductor using a discrete-port with a resistance of 1 kΩ.

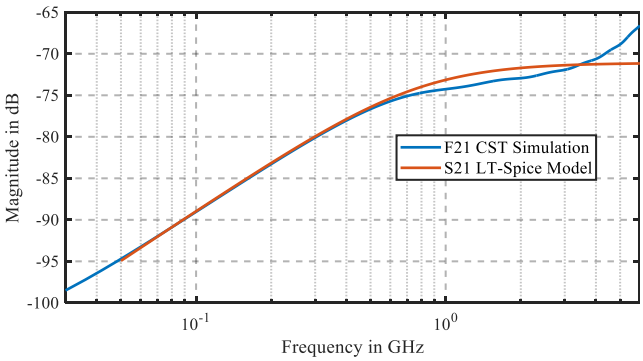

Fig. 5 Comparison between the frequency characteristic of the antenna using full wave simulation in CST with the RC lumped element model in SPICE.

D. Setup for ESD Localization

To measure the signals received by the antennas of the sensor, both ends of the cable are connected to an oscilloscope. A fast scope is needed to capture CDM like ESD signals with spectral content at least up to 3 GHz. In the setup an instrument with 40 GSa/s and an analog bandwidth of 12 GHz is used. Arranging the sensor in a serpentine increases the density of antennas in a certain area. Conductive fabric with a square resistance of 400 Ω is placed underneath the sensor. This underground avoids common-mode currents on the cable shield induced by the ESD. The material is connected to grounded via a 10 MΩ resistor. Later implementations my need other means to attenuate common mode currents on the outside of the cable. In Fig. 6 the setup for the localization is shown.

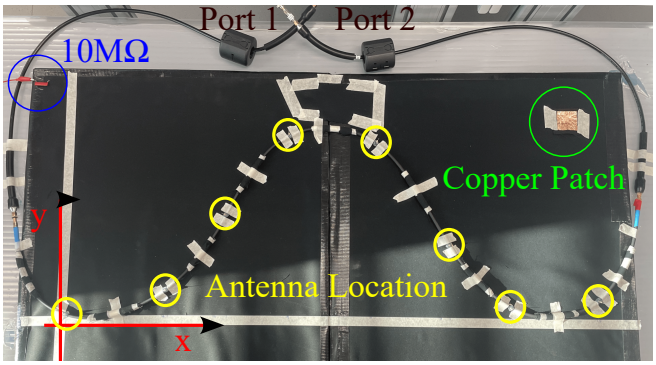

Fig. 6 Measurement setup for ESD event localization. Eight antennas are along a coax cable in serpentine shape. A coordinate system is defined for the sensor as shown. Both ends of the coax cable are connected to an oscilloscope.

As initial test, CDM like ESD events are generated by a charged person, dropping a metal sphere (20 mm) on a small copper patch (5 cm x 5 cm). A charge voltage of 1 kV is used for the measurement. Fig. 7 shows the waveforms captured for a ESD at the coordinates x = 1 m and y = 0.4 m. The signal arriving first at port 2 of the sensor, indicates that the ESD event is closer to port 2. The pulse-width of the received pulses is only 100 ps. Because antenna 8 is closest to the discharge, the largest amplitude can be observed at the first pulse. Antenna 7 and 6 are in very similar distance and therefore show very similar amplitudes. Starting at antenna 5 the interpretation is getting more difficult, since waveforms start to overlap. On port 2 the signals occur in reverse order and stronger attenuation.

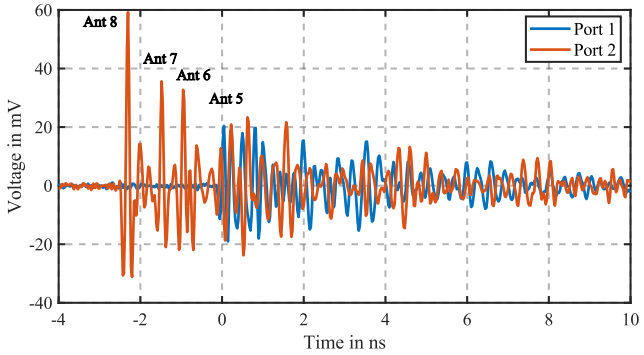

Fig. 7 Captured waveforms for an ESD event at x = 1 m and y = 0.4 m. Metal sphere with a diameter of 20 mm was charged to 1 kV and dropped on 5 cm x 5 cm copper patch.

III. Simulation Model and Reference Data

A. Sensor Model

A simulation model is generated and implemented in the simulation software LT-SPICE. This simulation model is later used to generate a set of reference data for the ESD localization. The main characteristics which have to be considered in the model are:

- Excitation signal (ESD source)
- Propagation delay from ESD source to receiving antenna
- Far field die-off α1/R
- Antenna characteristic
- Propagation delay of coax-cable
- Coax-cable attenuation

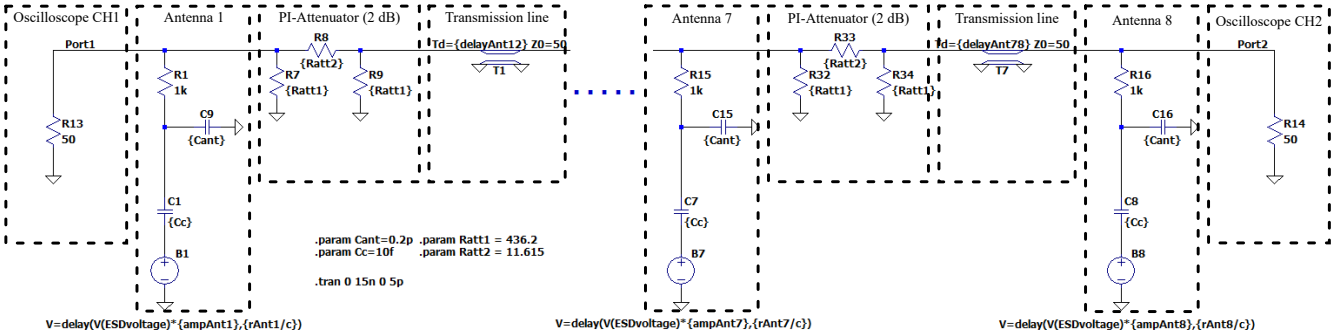

Fig. 8 LT-SPICE simulation model. The antennas use a 10 fF coupling capacitor and a 200 fF capacitance to ground to model the frequency characteristic. Cable losses are modeled using PI attenuators with 2 dB, the delay of the coax cable is added by ideal transmission lines. The delay of arrival from the ESD to the antenna and the 1/R die-off are modeled in the behavioral voltage source coupling to the antenna.

The excitation signal for the sensor is the electric field radiated by the CDM like ESD. CDM current waveforms and their corresponding radiated field have been analyzed in [9], [10]. In this model, a simple RLC circuit is excited by a voltage step and the corresponding current is used as waveform for the ESD voltage source. Fig. 9 shows the circuit and the corresponding waveform generated using a behavioral voltage source.

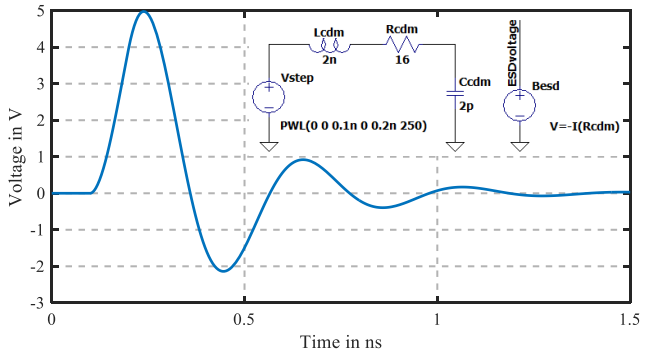

Fig. 9 CDM like ESD simulation excitation signal. The RLC circuit is excited with a voltage step with a rise-time of 100 ps and amplitude of 250 V. The voltage signal is defined using a behavioral voltage source with a voltage equal to the negative current through Rcdm.

To simulate the propagation delay from the ESD source to the individual antennas, the distance has to be known. Therefore the spatial coordinates of the antennas and the discharge are defined as parameters in the simulation. Using these coordinates the delay is calculated using:

$$t_{dA} = \frac{\|\vec{r}_{A\,ESD}\|}{c} \tag{2}$$

Where t_{dA} is the propagation time of the radiated signal from the ESD event to the antenna, with $\|\vec{r}_{A\,ESD}\|$ as the distance from the discharge to the antenna and c, the speed of light.

The 1/R far field die-off is considered as amplitude factor:

$$A_F = \frac{1}{\|\vec{r}_{A\,ESD}\|+0.001} \tag{3}$$

With A_F as amplitude factor, $\|\vec{r}_{A\,ESD}\|$ as the distance between antenna and ESD event. The position offset of 0.001 has been added to prevent division by zero in case an event is simulated exactly at the coordinate of an antenna. Both t_{dA} and A_F are included in the model of the antenna in the behavioral voltage source.

The antenna characteristic was modeled only by a capacitor to ground, whereby the signal is coupled to the antenna by a very small capacitor. Fig. 5 shows a good match between the LT-SPICE model and the full-wave simulation.

The propagation delay of the coax-cable has been obtained from TDR measurement and added to the model as ideal transmission line. A pi-attenuator with 2 dB has been added for each segment of transmission line between the antennas. This takes into account the losses of the cable at a frequency of around 3 GHz. Fig. 8 shows the SPICE model of the sensor.

B. *Reference Data Generation*

Since localization should be done using reference data from simulation, the response of the sensor has to be known for each possible discharge location. A transient simulation is performed for different spatial coordinates of the ESD source using LT-SPICE. The coordinates are varied on a 1.25 m x 1.5 m grid with step size of 1 cm. The maximal achievable localization resolution is determined by this step size. All time domain waveforms at the ports obtained from this simulation build the reference dataset.

IV. Localization Principle

The information about the location of the ESD event is in the time delay of the signals. This can be the time delay between sequential pulses seen on one port of the senser, but also delays between the both ports of the sensor. Hereby the amplitudes provide a weight function for evaluating the delay. Since the pulses have a complex overlap behavior the determination of time delay can be very difficult. The reference data set obtained from simulation models this complex behavior. It is used to compare the simulated waveforms with the measurement result using cross-correlation. The normalized cross-correlation between the simulated waveform of one port with the measured waveform at the same port is a measure of the similarity of the waveforms. This correlation is calculated for every grid point x,y. The coordinates which maximize this correlation, are expected to be the closest to the real ESD location:

$$\hat{R}_{SM}^{(x,y)}(\tau) = \int_{t_0}^{t_0+T} \frac{v_S^{(x,y)}(t-\tau)\, v_M(t)}{\sqrt{\hat{R}_{SS}^{(x,y)}(0)\, \hat{R}_{MM}(0)}}\, dt \tag{4}$$

Where $v_S^{(x,y)}$ is the simulated waveform at the coordinates x,y and v_M is the measured waveform. $\hat{R}_{SS}^{(x,y)}$ and $\hat{R}_{MM}$ are the autocorrelation functions of $v_S^{(x,y)}$ and v_M, which are used for the normalization. The result of this

equation is the correlation at one coordinate of the grid. Finding the maximum of $|\hat{R}_{SM}^{(x,y)}(\tau)|$ gives a measure for the similarity of the two waveforms. A coefficient describing this correlation between the simulation and measurement can be calculated by:

$$C_P{}^{(x,y)} = \max\left(\left|\hat{R}_{SM}^{(x,y)}(\tau)\right|\right) \tag{5}$$

With $C_P{}^{(x,y)}$ as correlation-coefficient and $\hat{R}_{SM}^{(x,y)}(\tau)$ as the normalized cross-correlation between simulation and measurement. The absolute value is used to neglect the polarity of the discharge. Fig. 10 and Fig. 11 show this correlation-coefficient for both ports, evaluated on the grid for a specific ESD event at x = 0.6 m and y = 0.25 m. In the result many local maxima are distributed all over the grid. These local maxima can appear even in large distance to the location of the discharge, since the correlation-coefficient does not take the time-delay between both ports into account.

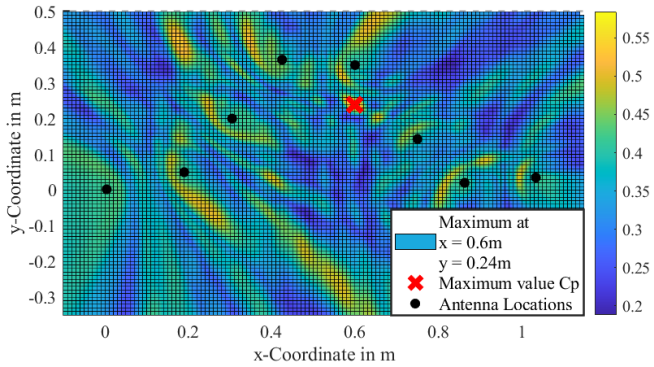

Fig. 10 $C_P{}^{(x,y)}$ calculated using port 1 of the sensor for each coordinate of the simulation grid for an ESD event at x = 0.6 m and y = 0.25 m.

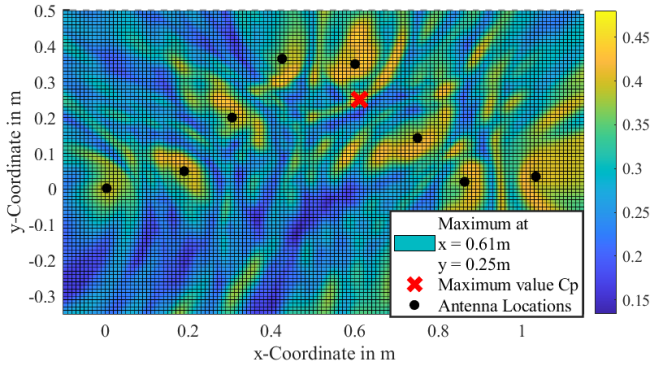

Fig. 11 $C_P{}^{(x,y)}$ calculated using port 2 of the sensor for each coordinate of the simulation grid for an ESD event at x = 0.6 m and y = 0.25 m.

The argument τ that maximizes $|\hat{R}_{SM}^{(x,y)}(\tau)|$, is the time shift between the simulated and measured waveforms. It depends on the systematic delay of the measurement and simulation. This time delay is given by:

$$t_d = \operatorname{argmax} \hat{R}_{SM}^{(x,y)}(\tau) \tag{6}$$

$$t_d = t_{d\,Sim} - t_{d\,Meas} \tag{7}$$

With t_d as systematic time delay between measured and simulated waveform. $t_{d\,Sim}$ and $t_{d\,Meas}$ are the time delays from the first data point to the start of the pulse. This delay must be identical for both ports, since the waveforms of the ports are captured at the same moment. Because this condition has to be fulfilled, the correlated waveforms of the ports are multiplied:

$$C_{PP}{}^{(x,y)} = \max\left(\hat{R}_{SM\,P1}^{(x,y)}(\tau) \circ \hat{R}_{SM\,P2}^{(x,y)}(\tau)\right) \tag{8}$$

Where $\hat{R}_{SM\,P1}^{(x,y)}(\tau)$ and $\hat{R}_{SM\,P2}^{(x,y)}(\tau)$ are the normalized cross-correlations between measurement and simulation of the corresponding port. $C_{PP}{}^{(x,y)}$ is measure for correlation including the constraint of equal time delay. Fig. 12 and Fig. 13 shows the result of Eq. 8 evaluated on the grid. Considering the delay between the ports by introducing the constraint for equal systematic delay greatly improves the location estimation. Only very few local maxima are visible and the estimated location is less than 1.5 cm off to the real event location.

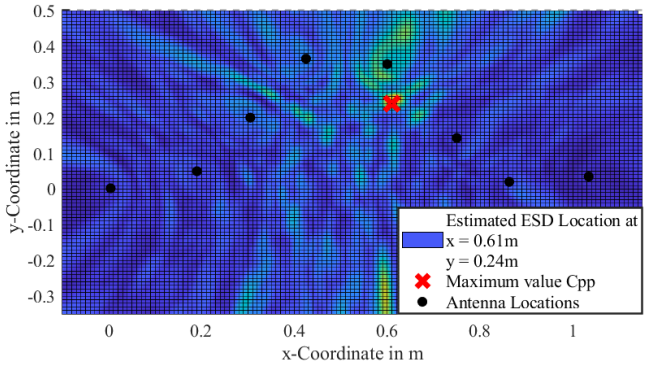

Fig. 12 $C_{PP}{}^{(x,y)}$ calculated over the whole simulation grid for an ESD event at x = 0.6 m and y = 0.25 m.

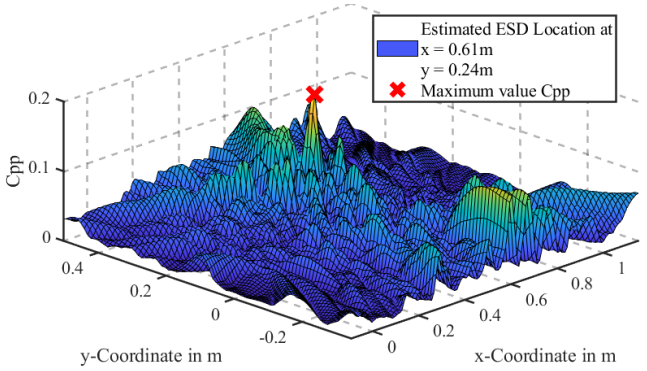

Fig. 13 $C_{PP}{}^{(x,y)}$ calculated over the whole simulation grid for an ESD event at x = 0.6 m and y = 0.25 m.

V. System Performance

The performance of this sensor and algorithm was tested at 3 different coordinates distributed on the simulation grid. An ESD was again generated by a person charged to 1 kV, dropping a 20 mm sphere on the 5 cm x 5 cm copper patch. The resulting signal to noise ratio, even without amplification at the sensors or the oscilloscope shows enough margin to detect even less than 100 V CDM pulses. For each coordinate 10 discharges have been recorded. In Fig. 14 the resulting estimations for the ESD event locations are shown. All estimated locations are very close or identical to the real discharge location. The worst location estimation is achieved for discharge location number three, with a maximal error of 5 cm. Fig. 15 shows the error of the ESD event localization in a boxplot. Here it should be mention, that the sphere has been

dropped by hand, which may also introduce a variation of 1 cm or more.

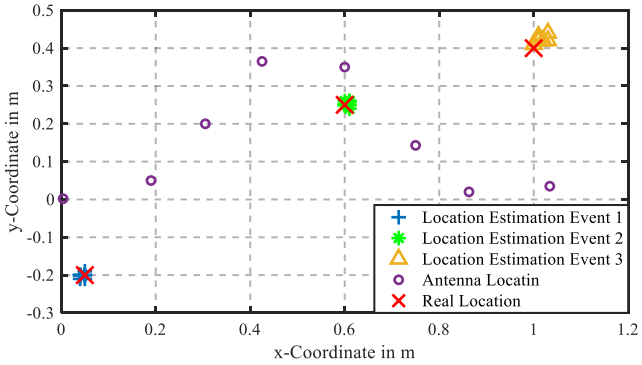

Fig. 14 Estimated locations for CDM like ESD events at x = 5 cm y = -20 cm, x = 60 cm y = 25 cm and x = 100 cm y = 40 cm

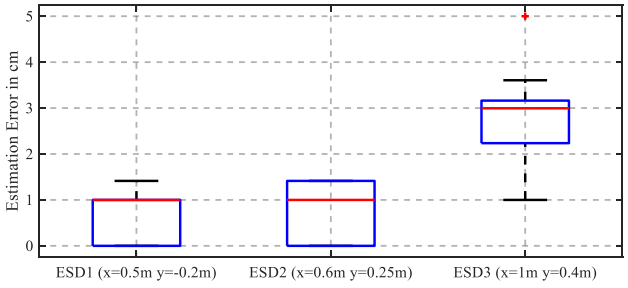

Fig. 15 Error of estimated ESD event locations for the system performance test. Each location includes 10 measurement results.

VI. Conclusion / Outlook

A novel sensor concept for the localization of CDM like ESD has been presented. The implementation using small wire antennas directly implanted in a coax-cable to detect signals at many locations. An oscilloscope detects signals from both ends and uses delay, magnitude and a SPICE based digital twin model to estimate the most likely discharge location. By spectral methods different ESD types, such as HBM, surface corona and CDM can be distinguished. The sensitivity can be increased by using local amplification at each sensor location such that low level CDM pulses of small ICs will become detectable.

Acknowledgment

The authors would like to thank Leonhard Petzel and Lucas Speckbacher for their input and valuable discussions.

References

[1] "White Paper 2: A Case for Lowering Component-level CDM ESD Specifications and Requirements," May 2021.

[2] S. Frei and D. Pomrnerenke, "About The Different Methods Of Observing Esd," in *Proceedings Electrical Overstress/Electrostatic Discharge Symposium*, 1997, pp. 117–124. doi: 10.1109/EOSESD.1997.634233.

[3] A. Steinman, J. Bernier, D. Boehm, T. Albano, W. Tan, and D. Pritchard, "Test methodologies for detecting ESD events in automated processing equipment," in *Electrical Overstress/Electrostatic Discharge Symposium Proceedings. 1999 (IEEE Cat. No.99TH8396)*, 1999, pp. 168–177. doi: 10.1109/EOSESD.1999.819003.

[4] A. Jahanzeb *et al.*, "Capturing real world ESD stress with event detector," in *EOS/ESD Symposium Proceedings*, 2011, pp. 1–5.

[5] K. Thongpull, N. Jindapetch, and W. Teerapabkajorndet, "Wireless ESD Event Locator Systems in Hard Disk Drive Manufacturing Environments," *IEEE Transactions on Industrial Electronics*, vol. 60, no. 11, pp. 5252–5259, Nov. 2013, doi: 10.1109/TIE.2012.2227911.

[6] D. L. Lin, L. F. DeChiaro, and M.-C. Jon, "A Robust ESD Event Locator System With Event Characterization," in *Proceedings Electrical Overstress/Electrostatic Discharge Symposium*, 1997, pp. 88–98. doi: 10.1109/EOSESD.1997.634230.

[7] J. Bernier, G. Croft, and R. Lowther, "Esd Sources Pinpointed By Analysis Of Radio Wave Emissions," in *Proceedings Electrical Overstress/Electrostatic Discharge Symposium*, 1997, pp. 83–87. doi: 10.1109/EOSESD.1997.634229.

[8] Q. Li, Y.-Z. Xie, K.-J. Li, and X. Kong, "A Portable Electric Field Detector With Precise Time Base for Transient Electromagnetic Radiation Source Location," *IEEE Trans Instrum Meas*, vol. 69, no. 4, pp. 1408–1415, Apr. 2020, doi: 10.1109/TIM.2019.2907775.

[9] T. J. Maloney, "Antenna Response to CDM E-fields," in *Electrical Overstress / Electrostatic Discharge Symposium Proceedings*, 2012, pp. 1–10.

[10] T. J. Maloney, "The Case for Measurement and Analysis of ESD Fields in Semiconductor Manufacturing," in *2018 IEEE Symposium on Electromagnetic Compatibility, Signal Integrity and Power Integrity (EMC, SI & PI)*, Jul. 2018, pp. 396–401. doi: 10.1109/EMCSI.2018.8495351.